Journal of Materials Chemistry

Cite this: J. Mater. Chem., 2012, 22, 21373

www.rsc.org/materials

COMMUNICATION

Green synthesis of Fe_3O_4 nanoparticles embedded in a porous carbon matrix and its use as anode material in Li-ion batteries†

Marcos Latorre-Sanchez, Ana Primo and Hermenegildo Garcia*

Received 26th July 2012, Accepted 6th September 2012
DOI: 10.1039/c2jm34978g

A scalable and simple process was developed for the preparation of Fe_3O_4 nanoparticles embedded in carbon using nontoxic and affordable materials. The resulting composite showed a high reversible capacity of 702 mA h g^{-1} as anode material in a Li-ion battery after 50 cycles.

Li-ion batteries are considered as one of the best technologies for reversible energy storage and can play in the future a major role as energy vector in transportation.[1–3] For this reason there is a continuous interest in improving the efficiency and developing more durable Li-ion batteries. One of the major research interests in Li-ion batteries has been the nature of the anode material.[4,5] Graphite has been widely employed for anode preparation but has as major limitation its low gravimetric capacity (372 mA h g^{-1}). Therefore there is still a need for investigating alternative materials that can eventually overcome the limited capacity of graphite.

In this context transition metal oxides have received considerable attention since they can exhibit about three times higher capacity than graphite.[6–8] This higher capacity is due to the different way in which lithium is incorporated into the anode. Thus, while in the case of graphite lithium becomes incorporated into the interlayer space (lithium intercalation), in the case of metal oxides it is accepted that a different mechanism denoted as "*conversion reaction*" takes place.[9] This conversion reaction consists in the storage of lithium as lithium oxide while the transition metal oxides form some metal domains. In this regard, one of the metal oxides that has been preferred in these studies is magnetite (Fe_3O_4) due to the lack of toxicity, availability and low cost of this iron oxide.[10–13] Eqn (1) summarizes the electrochemical reaction taking place between Fe_3O_4 and Li at the anode:

$$Fe_3O_4 + 8Li^+ + 8e^- \leftrightarrow 3Fe + 4Li_2O \quad (1)$$

This *conversion process* exhibits a theoretical capacity of 924 mA h g^{-1}. While the proof of principle of this Fe_3O_4 conversion has been already demonstrated there are still some practical problems that have to be solved before the system can be implemented at the commercial level. In particular, one of the major concerns in this anodic process is the large structural changes that occur during cycling which lead to remarkable variations in the volume and crystal structure that eventually produce a rapid decrease in the energy capacity.[9]

The two methodologies that have been reported to tackle with the durability and stability of the Fe_3O_4 films at the anode are complementary and are based on the use of nanoparticles (NPs) with small dimensions and large external surface area which facilitates reversible crystal changes and also the use of hybrid metal oxide–carbon composites.[14–16] Carbon in various forms improves the mechanical flexibility of the active Fe_3O_4 and at the same time ensures the electrical conductivity and reduces the resistance of the metal oxide.

There are several ways to form the Fe_3O_4 and carbon composites. One of these ways consists in the coating of the iron oxide NP with a carbon precursor that forming a shell coating the Fe_3O_4 NP will be subsequently converted into carbon with high electrical conductivity.[17,18] This procedure presents some advantages with respect to other more conventional methods such as the mechanical mixing of preformed Fe_3O_4 and carbons derived from the high contact area between the Fe_3O_4 phase and carbon. Other examples of Fe_3O_4–carbonaceous material composites applied in Li-ion batteries include the impregnation of porous carbons or the mixing of graphene layers with Fe_3O_4 precursors.[19–21] Common to all these precedents of Fe_3O_4–carbonaceous material composites is the need of lengthy protocols requiring the independent and previous preparation either of the carbon or of the Fe_3O_4.

In the present manuscript we report an innovative preparation procedure for a Fe_3O_4–carbon composite that is reliable, effects the simultaneous formation of Fe_3O_4 and carbon, uses affordable precursors and can be scaled up in a simple way. In fact, the present report constitutes a remarkable example of a sustainable process and valorization of biomass waste.

The preparation of the material (Fig. 1) starts with the precipitation of an alkaline alginate solution in water by dropwise addition into a $FeCl_3$ aqueous solution (see ESI† for Experimental details). As soon as the drops of alginate enter into the $FeCl_3$ solution beads of this biopolymer containing Fe^{3+} are formed and sediment at the bottom of the $FeCl_3$ solution. There are precedents in the literature describing similar precipitation of metal containing alginates.[22] In fact, alginates are widely used in water purification treatments to trap transition metal ions.[23,24] After formation of the hydrogel beads, water was gradually replaced by ethanol to form the corresponding alcogel before submitting the beads to supercritical CO_2 drying. This

Instituto Universitario de Tecnología Química, Univ. Politécnica de Valencia, Av. De los Naranjos s/n, 46022 Valencia, Spain. E-mail: hgarcia@qim.upv.es; Fax: +34 96 3877809

† Electronic supplementary information (ESI) available: Experimental section and Fig. S1–S5. See DOI: 10.1039/c2jm34978g

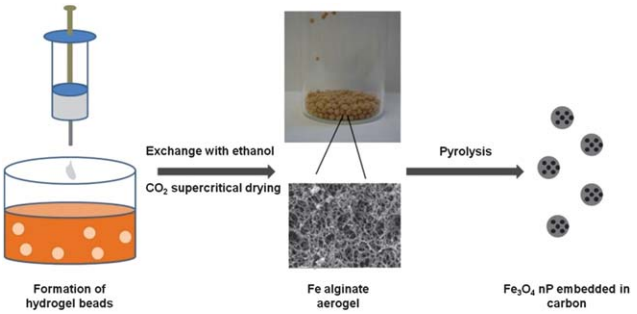

Fig. 1 Procedure for the preparation of the Fe_3O_4–C composite.

step of water removal by exchange with ethanol has been found essential for the success of supercritical CO_2 drying since supercritical CO_2 dissolves ethanol but is not miscible with water. As a result of this drying procedure a highly porous, high BET surface area (290 m^2 g^{-1}) iron containing alginate aerogel is obtained (Fe-alg). The iron content of Fe-alg determined by induced coupled plasma is 2.6 wt% and its morphology was assessed by scanning electron microscopy (SEM) (Fig. S1, ESI†). These Fe-alg beads were submitted to pyrolysis under argon atmosphere at 500 °C to form the Fe_3O_4–carbon composite (Fe_3O_4–C). It is known that polysaccharides undergo thermal decomposition towards graphitic carbons depending on the pyrolysis temperature.[25] Similar carbon materials as Fe_3O_4–C but using higher temperatures have been already used for supercapacitors.[26] In the present case we have maintained the pyrolysis temperature as low as possible to avoid the growth of Fe_3O_4 NPs and the chemical reduction of iron oxides to iron metal that has been reported to occur starting at 600 °C for other carbonaceous materials.[16] There are in the literature some precedents in which Fe_3O_4–carbon composites have also been obtained by pyrolysis of iron containing synthetic polymers such as polyacrylic acid or polyacrylonitrile,[16,27] but our method avoids the use of volatile organic compounds and toxic chemicals, makes use of affordable alginate that is valorized in this application and is carried out in aqueous media.

Fe_3O_4–C was characterized by a combination of techniques. The presence of magnetite NPs with small particle size was assessed by X-ray diffraction (XRD) of the powder (Fig. 2A) that, in addition, indicates the absence of iron metal (JCPDS card no. 19-629). Fe_3O_4 NPs are also observed by transmission electronic microscopy (TEM) that allows determination of a broad distribution of particles between 15 and 30 nm embedded in carbon (Fig. 2B and S2 in ESI†). The content of Fe_3O_4 in the Fe_3O_4–C composite was determined by thermogravimetry (Fig. S3 in ESI†), and was found to be 50.5 wt%. The morphology of the submillimetric beads Fe_3O_4–C was determined by SEM showing that the quasi spherical beads are highly porous and constituted of the agglomeration of small crystallites (Fig. 2C and S4 in ESI†). The formation of the carbon was assessed by Raman spectroscopy where the expected G band at 1590 cm^{-1} and a very broad D band peaking at 1350 cm^{-1} were recorded (Fig. 2D). In fact the very broad D band associated with defects can be deconvoluted into three components (D1, D3, D4). D1 and D4 (1358 and 1230 cm^{-1}, respectively) have been previously assigned to correspond to disordered graphite while D3 appearing at 1492 cm^{-1} is due to amorphous carbon.[28,29] Overall the Raman spectrum is compatible with pyrolysis of alginate forming a carbonaceous material tending to graphite (G band) but with a considerable level of disorder and accompanied by the presence of amorphous carbon. The BET surface area of Fe_3O_4–C is 620 m^2 g^{-1}, which is remarkably high for a composite containing about 50 wt% of Fe_3O_4.

Fe_3O_4–C was used as anode material to construct a Li-ion battery (see ESI†). Fig. 3A shows the first two cyclic voltammetry (CV) curves of this cell in the potential window of 0–3 V at a scan rate of 0.5 mV s^{-1}. These CV profiles and the observed variations upon cycling are in agreement with those previously reported in the literature for analogous Fe_3O_4–carbon materials and, therefore, can be interpreted similarly.[18,27] Thus, in the first scan the strong peak at 0.6 V must correspond to the reduction of Fe^{3+} and Fe^{2+} to Fe^0 accompanied by the irreversible reaction related to the decomposition of electrolyte. In the anodic part, the peak corresponding to the oxidation of Fe^0 to Fe^{3+} appears at 1.65 V. The second and subsequent scans show lower intensity of the cathodic and anodic peaks, which indicates capacity loss during the charging process.

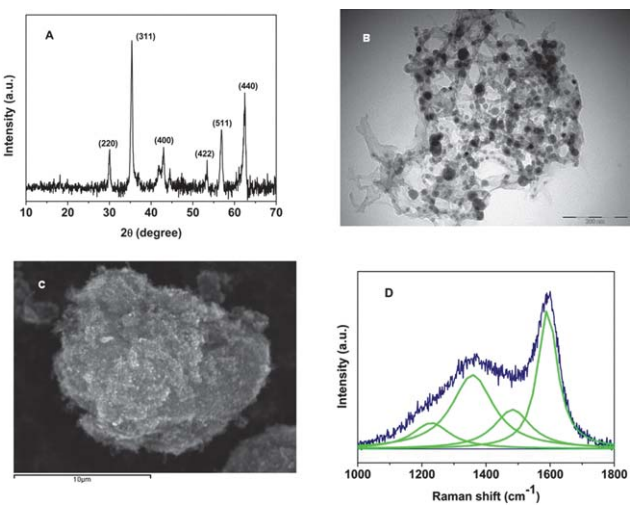

Fig. 2 (A) XRD pattern, (B) TEM image (scale bar: 200 nm), (C) SEM image (the scale bar corresponds to 10 microns) and (D) Raman spectrum of the Fe_3O_4–C composite.

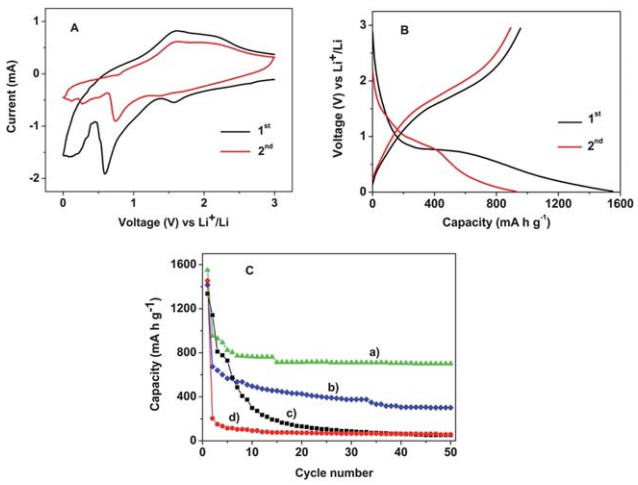

Fig. 3 (A) Cyclic voltammetry profiles and (B) galvanostatic discharge–charge curves for the first two cycles of the Fe_3O_4–C composite. (C) Cycling performance of (a) Fe_3O_4–C, (b) Fe_3O_4–CNT, (c) commercial Fe_3O_4 NP and (d) carbon made from pyrolysis of Ca-alg precursor.

Fig. 3B shows the discharge–charge profiles of the Fe_3O_4–C composite for the first two cycles. As can be seen in the figure the first discharge gives a capacity of 1550 mA h g^{-1} which is higher than the theoretical capacity of Fe_3O_4 (eqn (1)) and has been attributed to the formation of a solid–electrolyte interface film associated with the electrolyte decomposition and the formation of organic compounds with lithium as has been reported previously in the literature.[27,30] These chemical reactions are not observed in the second cycle where the charge capacity is about the theoretical value.

To characterize the cyclic performance of the Li-ion battery based on the Fe_3O_4–C composite as anode material we performed 50 cycles of charge and discharge (Fig. 3C) and compared the capacity of this battery with two other devices prepared using commercial Fe_3O_4 (<50 nm in size from Sigma-Aldrich) and carbon made from pyrolysis of Ca-alginate prepared following the same protocol as the one indicated in Fig. 1 but using Ca^{2+} instead of Fe^{3+} (Ca-alg). These measurements of charge–discharge cycles were carried out at a high current rate of 350 mA g^{-1} between the voltage limits of 0.01–3 V *vs.* Li^+/Li. The capacity value in Fig. 3C for Fe_3O_4–C has been calculated based on the mass of Fe_3O_4, because no significant contribution to the capacity is expected to be due to the presence of carbon. To support the absence of significant contribution to the capacity value by the carbon matrix containing iron oxide we performed analogous studies using pyrolyzed Ca-alg (80.4 wt% carbon content, determined by thermogravimetry under air atmosphere, Fig. S5 in ESI†) whereby no significant capacity was observed (see Fig. 3C, d)). Similarly, negligible capacities were measured for Li-ion batteries in which the anode was simply the carbonaceous residue obtained by pyrolysis of alginic acid under identical conditions. As can be seen in this figure, while commercial Fe_3O_4 NP loses capacity very rapidly upon cycling, Fe_3O_4–C composite shows a remarkable capacity retention to a high value of 702 mA h g^{-1} after 50 cycles that is much higher than the capacity of graphite and compares favorably with data reported in the literature for other Fe_3O_4–carbon composites.[14,15,17,19] To better put into context the performance of the Fe_3O_4–C hybrid material prepared here with those other Fe_3O_4–carbonaceous anodes reported in the literature we prepared a nanocomposite consisting of Fe_3O_4 NPs supported on multi-walled carbon nanotubes (Fe_3O_4–CNT) following a reported procedure[15] and tested this material as anode in a Li^+-ion battery under the same conditions. The results are shown in Fig. 3C and indicate the better performance of our Fe_3O_4–C material in spite of its much simpler and convenient preparation procedure.

Taking into account that the carbon content of Fe_3O_4–C is about 49.5 wt%, capacity values for the batteries containing this material considering the total mass are after 50 cycles about 355 mA h g^{-1}. Although the maximum iron content of the Fe_3O_4–C has a limit on the maximum Fe^{3+} uptake of alginate during the precipitation of Fe alginate (see Fig. 1) and is about the one that we have used for the preparation of the anodes in the present work, further optimization of the pyrolysis treatment leading to a more crystalline graphitic carbon accompanying Fe_3O_4 nanoparticles could probably increase the charge capacity value of the battery by allowing Li^+ ion intercalation also into the carbon host.

In conclusion, in the present work we have shown an innovative preparation of Fe_3O_4–carbon composite for application as Li-ion battery anode in which the formation of iron oxide NPs and carbon occurs simultaneously from a precursor characterized by a high surface area and porosity that is prepared by flocculation of alginate with a Fe^{3+} solution. This material complies with principles of green chemistry and represents a good example of biomass waste valorization reaching a performance in par with that of analogous materials obtained by more complex procedures and with less available precursors.

Notes and references

1 A. S. Arico, P. Bruce, B. Scrosati, J.-M. Tarascon and W. van Schalkwijk, *Nat. Mater.*, 2005, **4**, 366.
2 K. Kang, Y. S. Meng, J. Breger, C. P. Grey and G. Ceder, *Science*, 2006, **311**, 977.
3 M. Armand and J. M. Tarascon, *Nature*, 2008, **451**, 652.
4 J. L. Tirado, *Mater. Sci. Eng., R*, 2003, **40**, 103.
5 V. Etacheri, R. Marom, R. Elazari, G. Salitra and D. Aurbach, *Energy Environ. Sci.*, 2011, **4**, 3243.
6 P. Poizot, S. Laruelle, S. Grugeon, L. Dupont and J. M. Tarascon, *Nature*, 2000, **407**, 496.
7 Y. Yu, C.-H. Chen, J.-L. Shui and S. Xie, *Angew. Chem., Int. Ed.*, 2005, **44**, 7085.
8 D. Liu, B. B. Garcia, Q. Zhang, Q. Guo, Y. Zhang, S. Sepehri and G. Cao, *Adv. Funct. Mater.*, 2009, **19**, 1015.
9 J. Cabana, L. Monconduit, D. Larcher and M. R. Palacín, *Adv. Mater.*, 2010, **22**, E170.
10 P. L. Taberna, S. Mitra, P. Poizot, P. Simon and J. M. Tarascon, *Nat. Mater.*, 2006, **5**, 567.
11 C. Ban, Z. Wu, D. T. Gillaspie, L. Chen, Y. Yan, J. L. Blackburn and A. C. Dillon, *Adv. Mater.*, 2010, **22**, E145.
12 G. Zhou, D.-W. Wang, F. Li, L. Zhang, N. Li, Z.-S. Wu, L. Wen, G. Q. Lu and H.-M. Cheng, *Chem. Mater.*, 2010, **22**, 5306.
13 T. Zhu, J. S. Chen and X. W. Lou, *J. Phys. Chem. C*, 2011, **115**, 9814.
14 H. Liu, G. Wang, J. Wang and D. Wexler, *Electrochem. Commun.*, 2008, **10**, 1879.
15 Y. He, L. Huang, J.-S. Cai, X.-M. Zheng and S.-G. Sun, *Electrochim. Acta*, 2010, **55**, 1140.
16 Z. Yang, J. Shen and L. A. Archer, *J. Mater. Chem.*, 2011, **21**, 11092.
17 W.-M. Zhang, X.-L. Wu, J.-S. Hu, Y.-G. Guo and L.-J. Wan, *Adv. Funct. Mater.*, 2008, **18**, 3941.
18 Y. Piao, H. S. Kim, Y.-E. Sung and T. Hyeon, *Chem. Commun.*, 2010, **46**, 118.
19 M. Zhang, D. Lei, X. Yin, L. Chen, Q. Li, Y. Wang and T. Wang, *J. Mater. Chem.*, 2010, **20**, 5538.
20 T. Yoon, C. Chae, Y.-K. Sun, X. Zhao, H. H. Kung and J. K. Lee, *J. Mater. Chem.*, 2011, **21**, 17325.
21 S. K. Behera, *Chem. Commun.*, 2011, **47**, 10371.
22 G. Fundueanu, C. Nastruzzi, A. Carpov, J. Desbrieres and M. Rinaudo, *Biomaterials*, 1999, **20**, 1427.
23 T. A. Davis, B. Volesky and A. Mucci, *Water Res.*, 2003, **37**, 4311.
24 M. Arica, Gl. Bayramoglu, M. Yilmaz, S. Bektas and O. Genc, *J. Hazard. Mater.*, 2004, **109**, 191.
25 A. Gibaud, J. S. Xue and J. R. Dahn, *Carbon*, 1996, **34**, 499.
26 E. Raymundo-Piñero, F. Leroux and F. Béguin, *Adv. Mater.*, 2006, **18**, 1877.
27 J. S. Chen, Y. Zhang and X. W. Lou, *ACS Appl. Mater. Interfaces*, 2011, **3**, 3276.
28 F. Bonhomme, J. C. Lassegues and L. Servant, *J. Electrochem. Soc.*, 2001, **148**, E450.
29 A. Sadezky, H. Muckenhuber, H. Grothe, R. Niessner and U. Poschl, *Carbon*, 2005, **43**, 1731.
30 P. Verma, P. Maire and P. Novak, *Electrochim. Acta*, 2010, **55**, 6332.